Published in final edited form as:
J Mol Biol. 2012 September 28; 422(4): 532–544. doi:10.1016/j.jmb.2012.06.014.

Triepitopic antibody fusions inhibit cetuximab-resistant BRAF- and KRAS-mutant tumors via EGFR signal repression

Jamie B. Spangler[1], **Mandana T. Manzari**[2], **Elizabeth K. Rosalia**[3], **Tiffany F. Chen**[1], and **K. Dane Wittrup**[1,2,4,*]

Jamie B. Spangler: jamie.spangler@mit.edu; Mandana T. Manzari: manzari@mit.edu; Elizabeth K. Rosalia: erosalia@mit.edu; Tiffany F. Chen: tfenyi@mit.edu; K. Dane Wittrup: wittrup@mit.edu

[1]Department of Biological Engineering, MIT, 77 Massachusetts Avenue, Cambridge, MA 02139, USA

[2]Department of Chemical Engineering, MIT, 77 Massachusetts Avenue, Cambridge, MA 02139, USA

[3]Department of Biology, MIT, 77 Massachusetts Avenue, Cambridge, MA 02139, USA

[4]Koch Institute for Integrative Cancer Research, MIT, 77 Massachusetts Avenue, Cambridge, MA 02139, USA

Abstract

Dysregulation of epidermal growth factor receptor (EGFR) is a hallmark of many epithelial cancers, rendering this receptor an attractive target for cancer therapy. Much effort has been focused on the development of EGFR-directed antibody-based therapeutics, culminating in the clinical approval of the drugs cetuximab and panitumumab. Unfortunately, the clinical efficacy of these drugs has been disappointingly low and a particular challenge to targeting EGFR with antibody therapeutics has been resistance resulting from mutations in the downstream *raf* and *ras* effector proteins. Recent work demonstrating antibody cocktail-induced synergistic downregulation of EGFR motivated our design of cetuximab-based antibody-fibronectin domain fusion proteins that exploit downregulation-based EGFR inhibition by simultaneously targeting multiple receptor epitopes. We establish that amongst our engineered multiepitopic formats, trans-triepitopic antibody fusions demonstrate optimal efficacy, inducing rapid EGFR clustering and internalization, and consequently ablating downstream signaling. The combined effects of EGFR downregulation, ligand competition, and immune effector function conspire to inhibit tumor growth in xenograft models of cetuximab-resistant BRAF- and KRAS-mutant cancers. Our designed triepitopic constructs have the potential to enhance the efficacy and expand the scope of EGFR-directed therapies and our multiepitopic may be readily applied to other receptor targets to formulate a new class of antibody-based therapeutics.

*To whom correspondence should be addressed: Karl Dane Wittrup, 500 Main Street, 76-261D, Cambridge, MA 02139, USA, Phone: 617-253-4578, Fax: 617-452-3293, wittrup@mit.edu.

Keywords

Downregulation; Multispecific; Fibronectin; Cancer; ErbB1

Introduction

Epidermal growth factor receptor (EGFR) is a member of the ErbB family of receptor kinases that dimerizes following growth factor stimulation to induce receptor auto-phosphorylation and downstream signal activation, ultimately eliciting cellular responses such as migration, proliferation, and differentiation.[1] Dysregulation of EGFR signaling resulting from overexpression or mutation of either the receptor or its native ligands has been implicated in the pathogenesis of a host of epithelial-derived tumors,[2,3] motivating extensive drug design efforts that have led to the development of five approved EGFR-targeted drugs. Unfortunately, response rates have been disappointingly low and one of the major challenges to efficacy is the presence of mutations in signal effectors downstream of EGFR.[4] In particular, frequent mutations in the BRAF and KRAS genes,[5,6] which encode the mitogen-activated protein kinase (MAPK) effector *raf* and the MAPK and phosphoinositide 3 kinase (PI3K) effector *ras*, respectively, confer resistance to EGFR-targeted drugs,[7–9] necessitating development of more potent compounds that recruit additional inhibitory mechanisms such as receptor downregulation.

Accumulating evidence argues for the use of antibody cocktails targeting distinct epitopes on EGFR to cross-link or cluster and consequently downregulate receptor as a mechanism of inhibition (Fig. 1a), complementing conventional antibody mechanisms such as ligand competition.[10–12] Clustering might also be achieved with constructs that engage multiple epitopes on a single receptor. Bispecific nanobodies targeting two EGFR epitopes have been explored,[13] but higher order multiepitopic constructs introduce the geometric potential for two-dimensional surface cross-linking networks as opposed to strictly linear daisy chain formation, improving clustering efficiency to promote downregulation (Fig. 1b). We have performed a systematic evaluation of multiepitopic construct design and efficacy, engineering a series of novel fusion proteins based on the clinically approved antibody drug cetuximab (225) and determining the optimal specificity and topology for downregulation. Engineered triepitopic constructs rapidly cluster and internalize EGFR without agonizing the receptor. Furthermore, these constructs obstruct downstream signaling and inhibit tumor growth in models of 225-resistant cancers. In addition to informing enhanced anti-EGFR therapeutic design, our findings could represent a new class of antibody-based drugs targeting other surface proteins of therapeutic interest.

Results

We generated a panel of tri- and tetraepitopic constructs comprised of a full-length antibody linked to engineered EGFR-targeted variants of the tenth type III domain of human fibronectin (Fn3), a small (≈10 kDa), soluble beta-sandwich protein containing three hypervariable loops that confer target specificity.[14] We refer to the full constructs henceforth as Ab-Fn3 fusions and denote them by chain (heavy, H or light, L) and terminus

(N or C) of fusion. Prior work identified three non-competitive Fn3s which engage domain 1 (clone A), domain 3 (clone B), and domains 3 and 4 (clone D) of the EGFR ectodomain with sub-nanomolar affinity (Fig. S1).[15] Given three non-competitive Fn3 domains plus the 225 variable domain, we were able to design fusions capable of engaging up to four EGFR epitopes simultaneously. Ab-Fn3 fusions were designed with four different topologies: cis, trans, and double heavy chain (2HC) triepitopic fusions and tetraepitopic (tet) fusions (Fig. 2a). Previous combination antibody screens indicated improved downregulation when at least one ligand-competitive moiety was included,[12] prompting use of the epidermal growth factor (EGF)-competitive 225 immunoglobulin (IgG) scaffold. Use of the antibody backbone also imparts such benefits as straightforward recombinant expression, stability, and extended serum halflife.

Ab-Fn3 fusions are efficiently expressed from transiently transfected HEK 293 cells with high purity and yields of up to 10 mg/mL. We find that cis and trans fusions secrete best (Fig. S2a–b) and a representative dynamic light scattering profile of a trans-trispecific fusion confirms that the protein is of the expected monomeric size (Fig. S2c). Avidity enables five- to tenfold tighter EGFR binding of Ab-Fn3 fusions versus 225 (Table 1). The surface EGFR downregulatory activity of Ab-Fn3 fusions was compared to that of 225 or Fn3 on four EGFR-expressing cell lines with varying receptor densities (Table S1). As expected, the 225 antibody and monovalent Fn3s do not significantly impact surface EGFR levels, whereas Ab-Fn3 fusions downregulate receptor to varying extents depending on Fn3 orientation and fusion topology (Fig. 2b). The most effective formats for downregulation are trans and tet, distinguishing trans-triepitopics as optimal for both expression and downregulation. In addition to its dependence on Ab-Fn3 fusion format, downregulation efficacy is also dependent on the orientation and particular combination of Fn3 domains incorporated. Comprehensive analysis on 11 cell lines (Table S1) reveals HND+LCA as the most actively downregulating trans-triepitopic construct (Fig. 2c). This Ab-Fn3 fusion reproducibly achieves 80–90% surface EGFR reduction, motivating its selection for further characterization.

To demonstrate the advantage of designing higher order multiepitopic constructs, biepitopic Ab-Fn3 fusions were secreted in all four possible orientations (Fig. 2d). Constructs in the HN format are well expressed (Fig. S2d–e) and bind EGFR with enhanced affinity versus 225 (Table 1).

However, even the most active biepitopic Ab-Fn3 fusions downregulate EGFR to a lesser extent than tri- and tetraepitopic constructs, particularly the trans and tet fusions (Compare Fig. 2e to Fig. 2b), demonstrating the advantage of increased fusion construct valency in achieving receptor downregulation.

Receptor downregulation can be achieved via reduced synthesis rate, increased endocytic rate, decreased recycled fraction, or some combination thereof. We previously showed that antibody cocktails induce downregulation primarily through recycling inhibition; endocytosis rate is unchanged.[12] In contrast, trans-triepitopic treatment accelerates endocytosis to the same extent as EGF treatment (Figs. 3a, S3a) in addition to inhibiting

recycling (Fig. S3b), leading to more extensive downregulation than is attainable with antibody cocktail treatment.

To establish that downregulation corresponds with receptor clustering, we visualized HT-29 cells following treatment with our most active Ab-Fn3 fusion, HND+LCA. Deconvolution microscopy images reveal a dramatically punctate receptor distribution in the presence of Ab- Fn3 compared to 225, indicative of clustering (Fig. 3b). Isolation of *z*-sections through the HT-29 cell monolayer following treatment with the HND+LCA construct demonstrates that clusters are located both at the cell surface and intracellularly (Fig. S3c). In A549 cells, clusters appear within 9 minutes of treatment, increasing in size and quantity over time (Fig. 3c). We note similar receptor distribution patterns following treatment with other trans-triepitopic constructs, confirming rapid and efficient EGFR clustering (Fig. S3d).

Since ligand-mediated downregulation coincides with receptor activation, we examined whether Ab-Fn3 fusion-mediated downregulation was similarly agonistic. In-cell western analysis was performed for six known EGFR phosphosites including three major tyrosine autophosphorylation sites (Y1068, Y1148, and Y1173),[16] one minor autophosphorylation site (Y1086),[17] a Src tyrosine kinase target (Y845),[18] and a Ca-calmodulin-dependent kinase II target (S1046).[19] Studies were performed on the EGFR-dense A431 cell line, which exhibited 40–50% receptor downregulation following transtriepitopic fusion treatment. As shown in Fig. 4a, phosphorylation of the six sites increases in response to EGF stimulation, but none are activated by engineered fusion treatment during the same 2 h timecourse, despite the extensive clustering and downregulation we observe. Accordingly, effectors in the EGFR-driven PI3K pathway (Akt) and MAPK pathway (ERK) also show no phosphorylation in response to HND+LCA treatment (Fig. 4b–c). We conclude that despite its capacity to downregulate surface receptor, Ab-Fn3- induced clustering is insufficient to instigate EGFR activation.

We next posed the question of whether triepitopic constructs could antagonize growth factor- mediated activation downstream of EGFR. Our results demonstrate that EGF-induced Akt and ERK activation are delayed although not attenuated by 225, whereas signaling through both proteins is effectively abolished by Ab-Fn3 fusion treatment (Fig. 4d–e). Remarkably, these studies were performed in HT-29 cells, which express an activating mutant form of the MAPK effector *raf*, demonstrating that HND+LCA inhibits dysregulated downstream signaling through robust EGFR downregulation.

As a preliminary evaluation of the therapeutic potential of Ab-Fn3 fusions, we performed *in vitro* proliferation studies on our most active fusion, HND+LCA. To directly demonstrate the advantage of recruiting the additional mechanism of clustering to supplement EGFR ligand competition mediated by the unconjugated 225 antibody, we implemented proliferation studies in an autocrine ligand-expressing system. Autocrine expression of EGF and other EGFR ligands is frequently observed in tumor cells and can overwhelm exogenous therapeutics by increasing the apparent concentration of ligand, resulting in resistance to ligand-competitive antibodies, such as 225.[2,20–22] In an HMEC-derived cell line, denoted ECT, that aberrantly expresses chimeric EGF at a rate of 0.3 h^{-1} per 10^6 cells,[23] both 225 and the HND+LCA trans-triepitopic fusion are effective in inhibiting cell proliferation (Fig.

S4a). However, in the more aggressive TCT cell line, which secretes chimeric EGF at a rate of 0.6 h^{-1} per 10^6 cells,[23] 225 was unable to impair proliferation. In contrast, the HND +LCA trans-trispecific fusion reduces cell proliferation by 50% at saturating concentrations (tenfold higher than the equilibrium dissociation constant) (Fig. S4b).

Based on these promising *in vitro* results, we compared the therapeutic efficacy of the current standard of care 225 antibody to our engineered Ab-Fn3 fusion in mouse xenograft models. Their antibody-based structure allows Ab-Fn3 fusions to persist in the bloodstream with identical pharmacokinetics to 225 (Fig. 5a). We confirmed tumor targeting and perfusion of our Ab-Fn3 fusion construct via immunofluorescent staining of HT-29 tumor xenografts dissected from mice that were dosed 24 hours prior to sacrifice (Fig S5). *In vivo* efficacy of the most active transtriepitopic fusion (HND+LCA) was examined in four cell lines: A431, HT-29, HCT-116, and U87 (Fig. 5b). Compared to other cell lines, the A431 epidermoid carcinoma line exhibits less dramatic receptor downregulation following HND +LCA treatment and, accordingly, we observe no significant tumor control in xenograft models. Note that 225 was also ineffective against A431 xenografts at the concentration administered (10 mg/kg), consistent with previous findings.[24] However, in the BRAF mutant HT-29 colorectal carcinoma cell line, surface EGFR is potently downregulated by HND+LCA but not 225 and, correspondingly, xenograft tumor growth is inhibited by HND +LCA but not 225. In the KRAS mutant HCT-116 and wild-type BRAF and KRAS U87 cell lines, 225 moderately reduces surface EGFR levels, whereas HND+LCA induces more substantial downregulation. This behavior is predictive of *in vivo* efficacy, as 225 is partially controlling while HND+LCA effectively inhibits xenograft tumor growth.

Given the surprising result that EGFR-targeted Ab-Fn3 fusion treatment controls BRAF- and KRAS-mutant tumors, we further probed the therapeutic mechanism. Having established that downregulation correlates with tumor inhibition (Fig. 5b), we speculated that ligand competition also contributes to efficacy. To isolate the role of ligand obstruction, we designed an HND+LCA variant (HND+LCAx) with two 225 heavy chain variable domain mutations (Y102A and D103A) that weaken the 225-EGFR interaction by nearly thirtyfold (Fig. S6a).[25] Introduction of these mutations into HND+LCA results in approximately a tenfold drop in affinity, mitigated by the two Fn3 domains (Fig. S6b). Compared to HND+LCA, HND+LCAx competes sevenfold less efficiently with EGF (Fig. 6a).

We also parsed the contributions of immune effector function to tumor inhibition, as the role of immune cell recruitment via Fcγ receptor interaction in antibody efficacy has long been appreciated[26] and 225 is known to evoke antibody-mediated cellular cytotoxicity through Fc interaction with natural killer cells or macrophages.[27] We designed an HND+LCA variant (HND+LCAf) with a mutation in the IgG heavy chain constant region (D265A) that reduces binding to mouse FcγRIV by 96% (Fig. 6b)[28] without affecting antibody affinity or EGF competition (Fig. S6c–d). Ab-Fn3 fusion-induced clustering (Compare Fig. 6c to Fig. 3b) and downregulation (Fig. 6d) are intact for HND+LCAx and HND+LCAf, demonstrating isolation of ligand competition and effector function, respectively. As expected, the rate of receptor downregulation is reduced for HND+LCAx treatment (6.2 h^{-1}) compared to HND

+LCA treatment (12.8 h^{-1}) due to the tenfold decrease in affinity. However, the steady-state levels of downregulation for the two constructs differ by less than 10%.

We assessed the performance of HND+LCAx and HND+LCAf in mouse tumor xenograft models of the BRAF mutant HT-29 cell line, the KRAS mutant HCT-116 cell line, and the wild-type BRAF and KRAS U87 cell line (Fig. 7a). We found ligand inhibition to be requisite for tumor control in all three cell lines. In contrast, effector function was necessary for control of HT-29 but not HCT-116 or U87 xenografts. HT-29 tumors were dissected post-mortem and immunofluorescently stained for total EGFR content. Consistent with growth inhibition observations, HND+LCA-treated tumors express less EGFR than PBS- or HND+LCA variant- treated tumors (Fig. 7b).

Discussion

In summary, we introduce novel multiepitopic fusion constructs that utilize a clustering-based mechanism to downregulate and inhibit EGFR for therapeutic efficacy. Systematic evaluation of fusion topology identifies the trans-triepitopic format as optimal for expression and activity (Figs. 2, S2). The most active Ab-Fn3 fusion (HND+LCA) efficiently clusters and downregulates receptor (Fig. 3) in the absence of activation (Fig. 4b–c). It is notable that we achieve rapid receptor downregulation in the absence of agonism since fast endocytosis occurs exclusively through recruitment to clathrin-coated pits, which requires kinase activity.[29] Since Ab-Fn3 fusions do not stimulate phosphorylation, the internalization we observe presumably occurs slowly through basal membrane turnover or through lipid rafts.[30] We hypothesize that although the molecular rate of receptor internalization is not accelerated, clustered receptors are internalized synchronously, resulting in an apparent increase in the bulk endocytic rate constant following Ab-Fn3 fusion administration.

Unexpectedly, HND+LCA ablates PI3K and MAPK signaling even in the presence of a mutation downstream of EGFR (Fig. 4d–e). This may result from extreme sensitivity of the downstream effector response to the abundance of phosphorylated EGFR. Recently, Chen *et al.* showed that the incremental difference between 99% and 99.9% inhibition of EGFR activity translates into an 80% reduction in Akt and ERK activation.[31] The additional loss of EGFR activity via receptor downregulation compared to 225-mediated ligand competition alone could account for downstream inhibition we observe. BRAF mutation enhances *raf* kinase activity and KRAS mutation impairs the de-activating GTPase function of *ras*.[32,33] Our results therefore suggest that in both mutants, a non-zero level of EGFR-initiated upstream signal is necessary to propagate sufficient downstream signaling to drive tumor progression.

Finally, we establish the therapeutic efficacy of Ab-Fn3 fusion constructs in three different xenograft tumor models that resist 225 treatment, including one BRAF and one KRAS mutant cell line. Notably, we achieve robust control at a dose of 10 mg/kg with our triepitopic constructs, fivefold lower than the effective dose of the unconjugated 225 antibody.[24] We observe that *in vitro* downregulation is predictive of *in vivo* efficacy (Fig. 5b) and that receptor downregulation, ligand competition, and immune effector function all contribute to trans-triepitopic fusion efficacy (Fig. 7). Rapid formation of receptor-antibody

clusters on the surface of tumor cells could also enhance immune effector cell recruitment, potentiating antibody-dependent cellular cytotoxicity[27] or complement-dependent cytotoxicity, as was recently shown for antibody combinations;[34] however antibody effector function was not required for control of HCT-116 or U87 tumors.

In addition to the immediate potential therapeutic applications of EGFR-directed fusions in 225- refractory tumors, Ab-Fn3 fusions hold promise for targeted drug development. By enhancing the avidity of antibody-based constructs and introducing the complementary mechanism of cluster-induced downregulation, we may recover or improve the efficacy of existing drugs as well as design novel therapeutics that benefit from a multiepitopic strategy. Cluster-induced downregulation could also expand the indications of antibody-based therapeutics, as this mode of inhibition should remain effective in the face of receptor mutation and ligand dysregulation. Notably, Ab-Fn3 fusion treatment stifled growth of a 225-resistant in vitro model of ligand overexpression (Fig. S4b). The rapid and dramatic clustering effected by Ab-Fn3 fusions proposes their use for diagnostic purposes or as delivery vehicles for cell disruption agents such as toxins or siRNA. Further, the modularity of our Ab-Fn3 fusion constructs readily allows for development of drugs targeting other ErbB family members and receptor tyrosine kinases in general. Overall, the approach we present introduces a broadly applicable and effective concept for targeting, clustering, and downregulating a receptor to inhibit signaling and, ultimately, tumor growth.

Materials and Methods

Cell lines and antibodies

The transfected U87-SH,[31,32] ECT,[23] and TCT[23] cell lines were established as described previously[35,3635,3635,3635,3635,3635,36] and all other adherent cell lines were obtained from ATCC. HEK 293F cells were purchased from Invitrogen. Murine 225 monoclonal antibody was secreted from the commercially available hybridoma cell line (ATCC). Human 225 was secreted from transiently transfected HEK 293F cells. The H11 antibody was purchased through Lab Vision.

Adherent cells were maintained in their respective growth media (from ATCC unless otherwise indicated): DMEM for A431, U87-MG, U87-SH, BT-20, Hs578T, BT-549, and MDA-MB-231 cells, F-12K medium for A549 cells, McCoy's Modified 5A medium for HT-29 and HCT-116 cells, EMEM for HeLa cells, and HuMEC Ready Medium (Invitrogen) for HMEC, ECT, and TCT cells. U87-MG and U87-SH media were supplemented with 1 mM sodium pyruvate (Invitrogen) and 0.1 mM non-essential amino acids and transfected lines U87-SH were selected with 0.3 mM Geneticin (Invitrogen). To prepare complete culture media, ATCC formulations were supplemented with 10% fetal bovine serum (FBS) and 1X penicillin-streptomycin solution. All cell lines were maintained at 37°C with 5% ambient CO_2. HEK 293F cells were maintained in suspension in FreeStyle 293 expression medium (Invitrogen) at 37°C with 5% ambient CO_2. EGF (Sigma) was dosed at 20 nM. Trypsin-EDTA (Invitrogen) contains 0.05% trypsin and 0.5 mM EDTA.

Production of 225 and Ab-Fn3 fusions via HEK 293 cell transient transfection

The human IgG1 heavy and light chains of 225 or Ab-Fn3 fusions were inserted into the gWiz mammalian the 225 variable domains[37] and EGFR-binding fibronectin clones A, B, and D[15] were published previously. HEK 293F cells (Invitrogen) were grown to 1.2×10^6 cells per mL and diluted to 1×10^6 per mL. Miniprepped DNA (consisting of both the heavy and light chain constructs) and polyethyleneimine (Sigma) were independently diluted to 0.05 and 0.1 mg/mL in OptiPro medium, respectively, and incubated at room temperature for 15 min. Equal volumes of DNA and polyethyleneimine were mixed and incubated at room temperature for an additional 15 min. Subsequently, 500 mL of cells and 20 mL of DNA/polyethyleneimine mixture were added to a 2 L roller bottle and incubated at 37°, 5% CO_2 on a roller bottle adapter for seven days. The cell secretions were then centrifuged for 30 min at 15,000×g and the supernatant was purified via protein A affinity column chromatography (Thermo Fisher Scientific). Eluted constructs were concentrated, transferred to PBS, and characterized by sodium dodecyl sulfate polyacrylamide gel electrophoresis (SDS-PAGE) analysis.

Deconvolution microscopy

225 antibody and Ab-Fn3 fusions were labeled with Alexa 488 using a fluorescent labeling kit (Invitrogen). HT-29, A431, or A549 cells were plated at 50,000 per well in 8-well microscopy chambers and allowed to settle overnight. They were then serum- starved for 8–12 h and incubated with the appropriate antibody or Ab-Fn3 fusion construct for various time lengths at 37°C. Cells were immediately washed and resuspended in phenol red-free medium (Invitrogen) for imaging on a DeltaVision Spectris inverted deconvolution microscope (Applied Precision) at 60× magnification (oil immersion lens). For A549 images, wells were not washed but rather labeled constructs were added to phenol red-free medium and images were captured over a 30-minute time course. Deconvolution and projection of 0.15 μm z-slices as well as image analysis were performed using the SoftWoRx software package (Applied Precision). All compared images were acquired during a single session using identical settings.

Monensin recycling assays

U87 cells were seeded at 5×10^4 per well in 96-well plates, allowed to settle overnight, and serum starved for 12–16 h. They were then pre-incubated in basal medium with or without 200 μM monensin (Sigma), an inhibitor of receptor recycling,[38] at 37°C for 20 min. Either PBS or 20 nM trans-triepitopic Ab-Fn3 fusion was then added and incubation proceeded at 37°C. At each time point, cells were dissociated in trypsin-EDTA, acid stripped, and labeled for surface EGFR through incubation with 20 nM 225 for 1 h on ice. Cells were then washed and labeled with 66 nM PE-conjugated goat anti-mouse antibody (Invitrogen) for 20 min at 4°C. Cells were washed a final time and analyzed via flow cytometry.

Phospho-Akt and phospho-ERK immunoblot analysis

HT-29 cells were cultured to confluence in 6-well plates, allowed to settle overnight, and serum starved for 12 h. Cells were subsequently incubated with 20 nM isotype control antibody, 225, or the Ab-Fn3 fusion HND+LCA for the indicated length of time at 37°C.

For antagonism assays only, following 13 h incubation with PBS or 20 nM isotype control antibody, 225, or HND+LCA, 20 nM EGF was added and incubation proceeded at 37°C for the prescribed time length. Cell lysis was performed in 50 mM Tris•HCl, 2% SDS, 5% glycerol, 5 mM EDTA, 1 mM NaF, protease and phosphatase inhibitors (Thermo Fisher Scientific), 10 mM β-GP, 1 mM PMSF and 1 mM Na_3VO. Total protein levels were quantified for normalization via BCA assay (Thermo Fisher Scientific). Lysates were subsequently clarified by passage through centrifugal filter plates, separated via gel electrophoresis, subjected to SDS-PAGE analysis on 8% E-Page gels, and blotted onto nitrocellulose via iBlot apparatus (Invitrogen). The blotted membrane was then blocked in 1:1 PBS:Odyssey Blocking Buffer (Licor Biosciences) for 1 h at room temperature. Blots were incubated with 1:1000 dilutions of either anti-phosphoAkt S473 rabbit antibody or anti- phosphoERK1/2 Y202/Y204 rabbit antibody overnight at 4°C (Cell Signaling, Danvers, MA). A 1:15,000 dilution of mouse anti-beta actin antibody was added the next morning and incubation proceeded for 2 h. Following three washes, the membrane was incubated with goat anti-mouse (800 cw) and goat anti-rabbit (700 cw) near IR dye conjugate antibodies. After four additional washes, membranes were visualized on the Licor Odyssey infrared imaging system (Licor Biosciences). Phospho-Akt and phospho-ERK signals were normalized by beta actin signal for each lysate and all samples were normalized to a control lysate to ensure consistent intensity between blots. Image normalization and quantification were implemented with ImageJ software (NIH).

Cell Proliferation Assays

HMEC-derived TCT cells[23] were seeded at 3×10^3 per well in 96-well plates and allowed to adhere for 24 h. They were subsequently treated with 225 or the HND+LCA Ab-Fn3 fusion construct at the indicated concentrations in complete medium and incubated at 37°C for 72 h. Cell viability was assessed using the Wst1 tetrazolium salt cleavage assay (Roche)[39,40]. Relative proliferation was calculated as 450 nm absorbance relative to that of a PBS-treated control.

Pharmacokinetic studies

Antibody or Ab-Fn3 fusion was labeled with Licor 800cw near-infrared dye (Licor Biosciences). A total of 200 μg per mouse (10 mg/kg) of labeled antibody or Ab-Fn3 fusion suspended in 100 μL PBS was retro-orbitally injected into 6–8 week-old female Ncr *nu/nu* mice (three mice per cohort). At each time point, 20 μL blood was collected from the tail vein and maintained in a capillary tube. The blood was then centrifuged for 5 min at 1500×*g* to remove red blood cells and the plasma layer was transferred to a fresh capillary tube for analysis. Near-infrared signal was detected using the Licor Odyssey infrared imaging system at a wavelength of 800 nm. Signal was normalized to the first collection time point (immediately post-injection).

Mouse xenograft studies

A431 epidermoid carcinoma cells (2×10^6), HT-29 colorectal carcinoma cells (3×10^6), HCT-116 colorectal carcinoma cells (2×10^6), or U87 glioblastoma cells (3×10^6) were injected subcutaneously into the right flanks of 6–8 week-old female Ncr *nu/nu* mice. By

day 7 post-injection, tumors had grown to a minimum volume of 20 mm^3. Mice were randomized and retro-orbital injections of PBS or 10 mg/kg 225, HND+LCA, HND+LCAx, or HND+LCAf were carried out for the duration of the experiment (with the exception of U87 tumors, which were treated only through day 31). Tumor volume was monitored daily with a digital caliper using the formula Volume = $0.5\times(\text{Length})\times(\text{Width})^2$ although not all points are shown to enhance figure clarity. Throughout the experiment, mice were monitored for overall health and activity in accordance with Massachusetts Institute of Technology Committee on Animal Care protocol number 0509-048-12. Each cohort included three or four mice.

Yeast-Displayed Fcγ Receptor Binding Assay

Transformed yeast stably displaying the extracellular domain of Fcγ receptor I (residues 25–297), II (residues 30–207), III (residues 31–215), or IV (residues 21–203) followed by a cmyc tag were incubated with 100 nM antibody or Ab-Fn3 fusion construct for 30 min at room temperature. Chicken anti-cmyc antibody (Invitrogen) was also added to detect properly displayed receptor. Yeast cells were then washed and goat anti-human 488-labeled secondary antibody (Invitrogen) was added to detect bound IgG fusion. Concurrently, goat anti-chicken 647-labeled secondary antibody (Invitrogen) was added to detect cmyc. Cells were incubated at 4°C for 15 min, washed, and then analyzed on a FACS Calibur flow cytometer (BD Biosciences). Mean bound Ab-Fn3 fusion fluorescence is reported for functionally displaying (cmyc positive) yeast.

Tumor immunofluorescence studies

HT-29 tumor xenografts were dissected on day 38 post- inoculation (24 h after the final therapeutic injection), immersed in optimal cutting temperature freezing medium, and flash frozen with liquid nitrogen in a bath of 2-methylbutane (Sigma). Tumors were subsequently sectioned (7 μm slices) in a cryostat and affixed to slides. For immunofluorescent staining, slides were fixed with formalin for 10 min and then washed three times with PBS. Cells were subsequently permeabilized in PBS containing 0.1% Triton X-100 for 10 min and washed three additional times. Blocking with a 5% solution of goat serum (Invitrogen) proceeded for 1 h at room temperature, followed by overnight incubation with 20 nM polyclonal rabbit anti-EGFR antibody (Abcam, Cambridge, MA) or 20 nM rabbit anti-human Fc antibody (Invitrogen) in 5% goat serum at 4°C. Slides were rinsed three times and incubated with 33 nM goat anti-rabbit 488-conjugated antibody (Invitrogen) in PBS containing 0.1% Tween 20 for 1 h at room temperature. Following four final PBS washes, slides were incubated with the double-stranded DNA stain DAPI (Sigma) for one minute at room temperature, mounted with Vectashield (Vector Laboratories), and sealed with clear nail polish. Imaging was performed on a DeltaVision Spectris microscope (Applied Precision) at 10× magnification. Image acquisition and processing were conducted using the SoftWoRx software package. The images were stitched from a series of panels acquired in a single plane of focus. All images presented were captured during a single microscopy session using identical intensity settings. Brightness and contrast were normalized using ImageJ software (NIH).

Statistical analysis

One-way repeated measures ANOVA was performed on mouse xenograft data to compare PBS, 225, and trans-triepitopic Ab-Fn3 treatments. The algorithm was implemented in MATLAB (Mathworks).

Affinity titrations, receptor quantification, receptor downregulation assays, monensin-based recycling studies, in cell western assays, and EGF competition analyses were performed as described previously.[12,15]

Supplementary Material

Refer to Web version on PubMed Central for supplementary material.

Acknowledgments

We thank Eliza Vasile of the Swanson Biotechnology Center for expert technical assistance. This research was supported by NIH grant CA96504 and an NDSEG Fellowship to JBS.

Abbreviations

EGFR	Epidermal growth factor receptor
MAPK	Mitogen-activated protein kinase
PI3K	Phosphoinositide 3 kinase
Fn3	Tenth type III domain of human fibronectin
Ab-Fn3	Antibody-fibronectin domain fusion
EGF	Epidermal growth factor
ERK1/2	extracellular signal-regulated protein kinases 1 and 2
DMEM	Dulbecco’s modified Eagle medium
EDTA	ethylenediaminetetraacetic acid
PBS	phosphate buffered saline
PBSA	phosphate buffered saline containing 0.1% bovine serum albumin
SDS-PAGE	sodium dodecyl sulfate polyacrylamide gel electrophoresis

References

1. Yarden Y, Sliwkowski MX. Untangling the ErbB signalling network. Nat Rev Mol Cell Biol. 2001; 2:127–37. [PubMed: 11252954]
2. Salomon DS, Brandt R, Ciardiello F, Normanno N. Epidermal growth factor-related peptides and their receptors in human malignancies. Crit Rev Oncol Hematol. 1995; 19:183–232. [PubMed: 7612182]
3. Nicholson RI, Gee JM, Harper ME. EGFR and cancer prognosis. Eur J Cancer. 2001; 37(Suppl 4):S9–15. [PubMed: 11597399]
4. Martinelli E, De Palma R, Orditura M, De Vita F, Ciardiello F. Anti-epidermal growth factor receptor monoclonal antibodies in cancer therapy. Clin Exp Immunol. 2009; 158:1–9. [PubMed: 19737224]

5. Bollag G, McCormick F. Regulators and effectors of ras proteins. Annu Rev Cell Biol. 1991; 7:601–32. [PubMed: 1667084]
6. Vakiani E, Solit DB. KRAS and BRAF: drug targets and predictive biomarkers. J Pathol. 2011; 223:219–29. [PubMed: 21125676]
7. Lievre A, Bachet JB, Le Corre D, Boige V, Landi B, Emile JF, Cote JF, Tomasic G, Penna C, Ducreux M, Rougier P, Penault-Llorca F, Laurent-Puig P. KRAS mutation status is predictive of response to cetuximab therapy in colorectal cancer. Cancer Res. 2006; 66:3992–5. [PubMed: 16618717]
8. Amado RG, Wolf M, Peeters M, Van Cutsem E, Siena S, Freeman DJ, Juan T, Sikorski R, Suggs S, Radinsky R, Patterson SD, Chang DD. Wild-type KRAS is required for panitumumab efficacy in patients with metastatic colorectal cancer. J Clin Oncol. 2008; 26:1626–34. [PubMed: 18316791]
9. Di Nicolantonio F, Martini M, Molinari F, Sartore-Bianchi A, Arena S, Saletti P, De Dosso S, Mazzucchelli L, Frattini M, Siena S, Bardelli A. Wild-type BRAF is required for response to panitumumab or cetuximab in metastatic colorectal cancer. J Clin Oncol. 2008; 26:5705–12. [PubMed: 19001320]
10. Friedman LM, Rinon A, Schechter B, Lyass L, Lavi S, Bacus SS, Sela M, Yarden Y. Synergistic down-regulation of receptor tyrosine kinases by combinations of mAbs: implications for cancer immunotherapy. Proc Natl Acad Sci U S A. 2005; 102:1915–20. [PubMed: 15684082]
11. Pedersen MW, Jacobsen HJ, Koefoed K, Hey A, Pyke C, Haurum JS, Kragh M. Sym004: a novel synergistic anti-epidermal growth factor receptor antibody mixture with superior anticancer efficacy. Cancer Res. 2010; 70:588–97. [PubMed: 20068188]
12. Spangler JB, Neil JR, Abramovitch S, Yarden Y, White FM, Lauffenburger DA, Wittrup KD. Combination antibody treatment down-regulates epidermal growth factor receptor by inhibiting endosomal recycling. Proc Natl Acad Sci U S A. 2010; 107:13252–7. [PubMed: 20616078]
13. Roovers RC, Vosjan MJ, Laeremans T, El Khoulati R, de Bruin RC, Ferguson KM, Verkleij AJ, van Dongen GA, van Bergen En Henegouwen PM. A bi-paratopic anti-EGFR nanobody efficiently inhibits solid tumour growth. Int J Cancer. 2011
14. Koide A, Koide S. Monobodies: antibody mimics based on the scaffold of the fibronectin type III domain. Methods Mol Biol. 2007; 352:95–109. [PubMed: 17041261]
15. Hackel BJ, Neil JR, White FM, Wittrup KD. Epidermal growth factor receptor downregulation by small heterodimeric binding proteins. Protein engineering, design & selection: PEDS. 2012; 25:47–57.
16. Downward J, Waterfield MD, Parker PJ. Autophosphorylation and protein kinase C phosphorylation of the epidermal growth factor receptor. Effect on tyrosine kinase activity and ligand binding affinity. J Biol Chem. 1985; 260:14538–46. [PubMed: 2997213]
17. Margolis BL, Lax I, Kris R, Dombalagian M, Honegger AM, Howk R, Givol D, Ullrich A, Schlessinger J. All autophosphorylation sites of epidermal growth factor (EGF) receptor and HER2/neu are located in their carboxyl-terminal tails. Identification of a novel site in EGF receptor. J Biol Chem. 1989; 264:10667–71. [PubMed: 2543678]
18. Sato K, Sato A, Aoto M, Fukami Y. c-Src phosphorylates epidermal growth factor receptor on tyrosine 845. Biochem Biophys Res Commun. 1995; 215:1078–87. [PubMed: 7488034]
19. Countaway JL, Nairn AC, Davis RJ. Mechanism of desensitization of the epidermal growth factor receptor protein-tyrosine kinase. J Biol Chem. 1992; 267:1129–40. [PubMed: 1309762]
20. Kuwada SK, Lund KA, Li XF, Cliften P, Amsler K, Opresko LK, Wiley HS. Differential signaling and regulation of apical vs. basolateral EGFR in polarized epithelial cells. Am J Physiol. 1998; 275:C1419–28. [PubMed: 9843701]
21. Normanno N, Bianco C, De Luca A, Maiello MR, Salomon DS. Target-based agents against ErbB receptors and their ligands: a novel approach to cancer treatment. Endocr Relat Cancer. 2003; 10:1–21. [PubMed: 12653668]
22. Normanno N, Bianco C, Strizzi L, Mancino M, Maiello MR, De Luca A, Caponigro F, Salomon DS. The ErbB receptors and their ligands in cancer: an overview. Curr Drug Targets. 2005; 6:243–57. [PubMed: 15857286]

23. Joslin EJ, Opresko LK, Wells A, Wiley HS, Lauffenburger DA. EGF-receptor-mediated mammary epithelial cell migration is driven by sustained ERK signaling from autocrine stimulation. Journal of cell science. 2007; 120:3688–99. [PubMed: 17895366]
24. Goldstein NI, Prewett M, Zuklys K, Rockwell P, Mendelsohn J. Biological efficacy of a chimeric antibody to the epidermal growth factor receptor in a human tumor xenograft model. Clinical cancer research: an official journal of the American Association for Cancer Research. 1995; 1:1311–8. [PubMed: 9815926]
25. Li S, Schmitz KR, Jeffrey PD, Wiltzius JJ, Kussie P, Ferguson KM. Structural basis for inhibition of the epidermal growth factor receptor by cetuximab. Cancer Cell. 2005; 7:301–11. [PubMed: 15837620]
26. Griggs J, Zinkewich-Peotti K. The state of the art: immune-mediated mechanisms of monoclonal antibodies in cancer therapy. Br J Cancer. 2009; 101:1807–12. [PubMed: 19809433]
27. Zhang W, Gordon M, Schultheis AM, Yang DY, Nagashima F, Azuma M, Chang HM, Borucka E, Lurje G, Sherrod AE, Iqbal S, Groshen S, Lenz HJ. FCGR2A and FCGR3A polymorphisms associated with clinical outcome of epidermal growth factor receptor expressing metastatic colorectal cancer patients treated with single-agent cetuximab. J Clin Oncol. 2007; 25:3712–8. [PubMed: 17704420]
28. Shields RL, Namenuk AK, Hong K, Meng YG, Rae J, Briggs J, Xie D, Lai J, Stadlen A, Li B, Fox JA, Presta LG. High resolution mapping of the binding site on human IgG1 for Fc gamma RI, Fc gamma RII, Fc gamma RIII, and FcRn and design of IgG1 variants with improved binding to the Fc gamma R. J Biol Chem. 2001; 276:6591–604. [PubMed: 11096108]
29. Sorkin A, Goh LK. Endocytosis and intracellular trafficking of ErbBs. Exp Cell Res. 2009; 315:683–96. [PubMed: 19278030]
30. Zhu JX, Goldoni S, Bix G, Owens RT, McQuillan DJ, Reed CC, Iozzo RV. Decorin evokes protracted internalization and degradation of the epidermal growth factor receptor via caveolar endocytosis. J Biol Chem. 2005; 280:32468–79. [PubMed: 15994311]
31. Chen WW, Schoeberl B, Jasper PJ, Niepel M, Nielsen UB, Lauffenburger DA, Sorger PK. Input-output behavior of ErbB signaling pathways as revealed by a mass action model trained against dynamic data. Mol Syst Biol. 2009; 5:239. [PubMed: 19156131]
32. Scheffzek K, Ahmadian MR, Kabsch W, Wiesmuller L, Lautwein A, Schmitz F, Wittinghofer A. The Ras-RasGAP complex: structural basis for GTPase activation and its loss in oncogenic Ras mutants. Science. 1997; 277:333–8. [PubMed: 9219684]
33. Wan PT, Garnett MJ, Roe SM, Lee S, Niculescu-Duvaz D, Good VM, Jones CM, Marshall CJ, Springer CJ, Barford D, Marais R. Mechanism of activation of the RAF-ERK signaling pathway by oncogenic mutations of B-RAF. Cell. 2004; 116:855–67. [PubMed: 15035987]
34. Dechant M, Weisner W, Berger S, Peipp M, Beyer T, Schneider-Merck T, Lammerts van Bueren JJ, Bleeker WK, Parren PW, van de Winkel JG, Valerius T. Complement-dependent tumor cell lysis triggered by combinations of epidermal growth factor receptor antibodies. Cancer Res. 2008; 68:4998–5003. [PubMed: 18593896]
35. Huang HS, Nagane M, Klingbeil CK, Lin H, Nishikawa R, Ji XD, Huang CM, Gill GN, Wiley HS, Cavenee WK. The enhanced tumorigenic activity of a mutant epidermal growth factor receptor common in human cancers is mediated by threshold levels of constitutive tyrosine phosphorylation and unattenuated signaling. J Biol Chem. 1997; 272:2927–35. [PubMed: 9006938]
36. Huang PH, Mukasa A, Bonavia R, Flynn RA, Brewer ZE, Cavenee WK, Furnari FB, White FM. Quantitative analysis of EGFRvIII cellular signaling networks reveals a combinatorial therapeutic strategy for glioblastoma. Proc Natl Acad Sci U S A. 2007; 104:12867–72. [PubMed: 17646646]
37. Mendelsohn J. Epidermal growth factor receptor inhibition by a monoclonal antibody as anticancer therapy. Clin Cancer Res. 1997; 3:2703–7. [PubMed: 10068277]
38. Basu SK, Goldstein JL, Anderson RG, Brown MS. Monensin interrupts the recycling of low density lipoprotein receptors in human fibroblasts. Cell. 1981; 24:493–502. [PubMed: 6263497]
39. Ishiyama M, Tominaga H, Shiga M, Sasamoto K, Ohkura Y, Ueno K. A combined assay of cell viability and in vitro cytotoxicity with a highly water-soluble tetrazolium salt, neutral red and crystal violet. Biol Pharm Bull. 1996; 19:1518–20. [PubMed: 8951178]

40. Hamasaki K, Kogure K, Ohwada K. A biological method for the quantitative measurement of tetrodotoxin (TTX): tissue culture bioassay in combination with a water-soluble tetrazolium salt. Toxicon. 1996; 34:490–5. [PubMed: 8735249]

Highlights

- Anti-EGFR therapeutics are ineffective in cancers with downstream signaling mutations
- Engineered antibodies targeting multiple EGFR epitopes downregulate surface receptor
- Downregulation abrogates signaling, even in the presence of downstream mutations
- Engineered antibodies inhibit growth of tumor xenografts with signaling mutations
- Constructs show therapeutic potential and multiepitopic strategy informs drug design

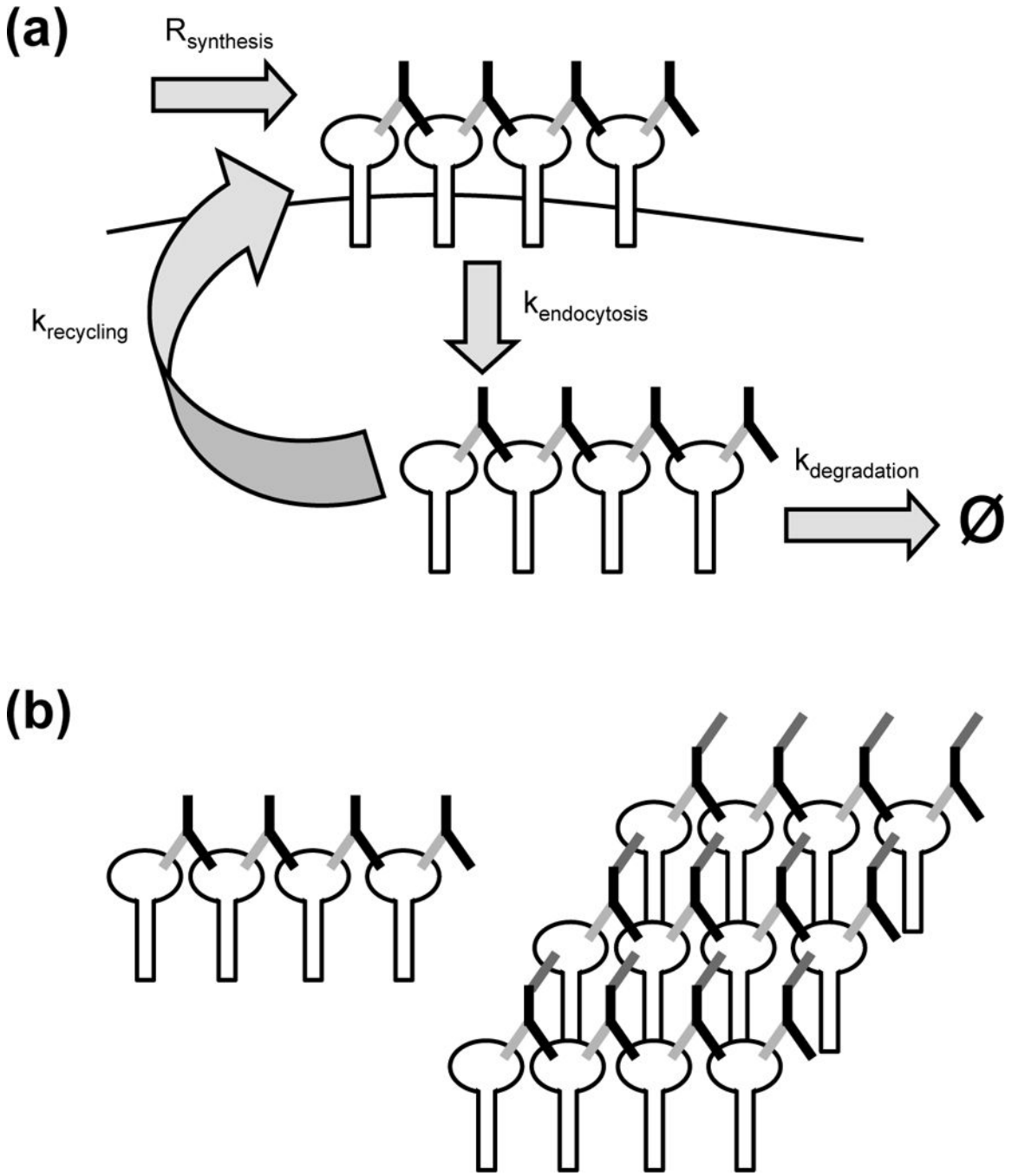

Fig. 1.

EGFR trafficking response to multiepitopic antibody-induced clustering. **(a)** A basic model of receptor clustering and trafficking following treatment with a bispecific antibody targeting two non-overlapping epitopes on EGFR is shown. Note that in contrast to the requirement for two monoclonal antibodies to propagate crosslinking, a single multiepitopic construct can efficiently cluster surface receptor. Receptor is synthesized with a rate $R_{synthesis}$, internalized with rate $k_{endocytosis}$, recycled back to the surface with rate $k_{recycling}$, and degraded with rate $k_{degradation}$. **(b)** Comparison of cross-linking by biepitopic (left) and

triepitopic (right) constructs illustrates the advantage of designing higher order multiepitopic antibodies. Whereas biepitopic antibodies are limited to formation of one-dimensional linear cross-linked complexes, antibodies that engage three or more epitopes can form two-dimensional surface meshworks of cross-linked antibody-receptor complexes.

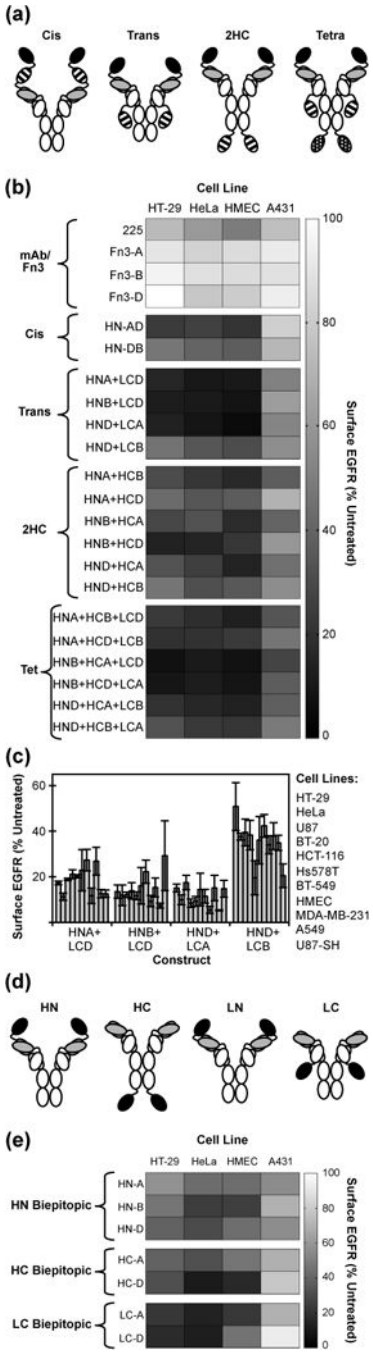

Fig. 2.

Multiepitopic constructs induce EGFR downregulation. **(a)** Schematic diagram of the four engineered tri- and tetraepitopic Ab-Fn3 fusions, consisting of the 225 human IgG1 constant (white) and variable (gray) domains fused to multiple Fn3s (black and patterned). **(b)** Heat map displaying surface EGFR downregulation on four cell lines following 13 h incubation with the indicated constructs. Percent surface receptor remaining relative to an untreated control is depicted. **(c)** Direct comparison of 13 h EGFR downregulation on eleven cell lines by the four trans-triepitopic constructs. Error bars represent the standard deviation from

three replicate experiments. **(d)** Orientation of the four possible biepitopic Ab-Fn3 fusion topologies, including the 225 IgG1 (colored as in **a**) fused to one Fn3 (black) at the heavy or light chain N or C terminus. **(e)** Surface EGFR downregulation heat maps (13 h) for biepitopic constructs.

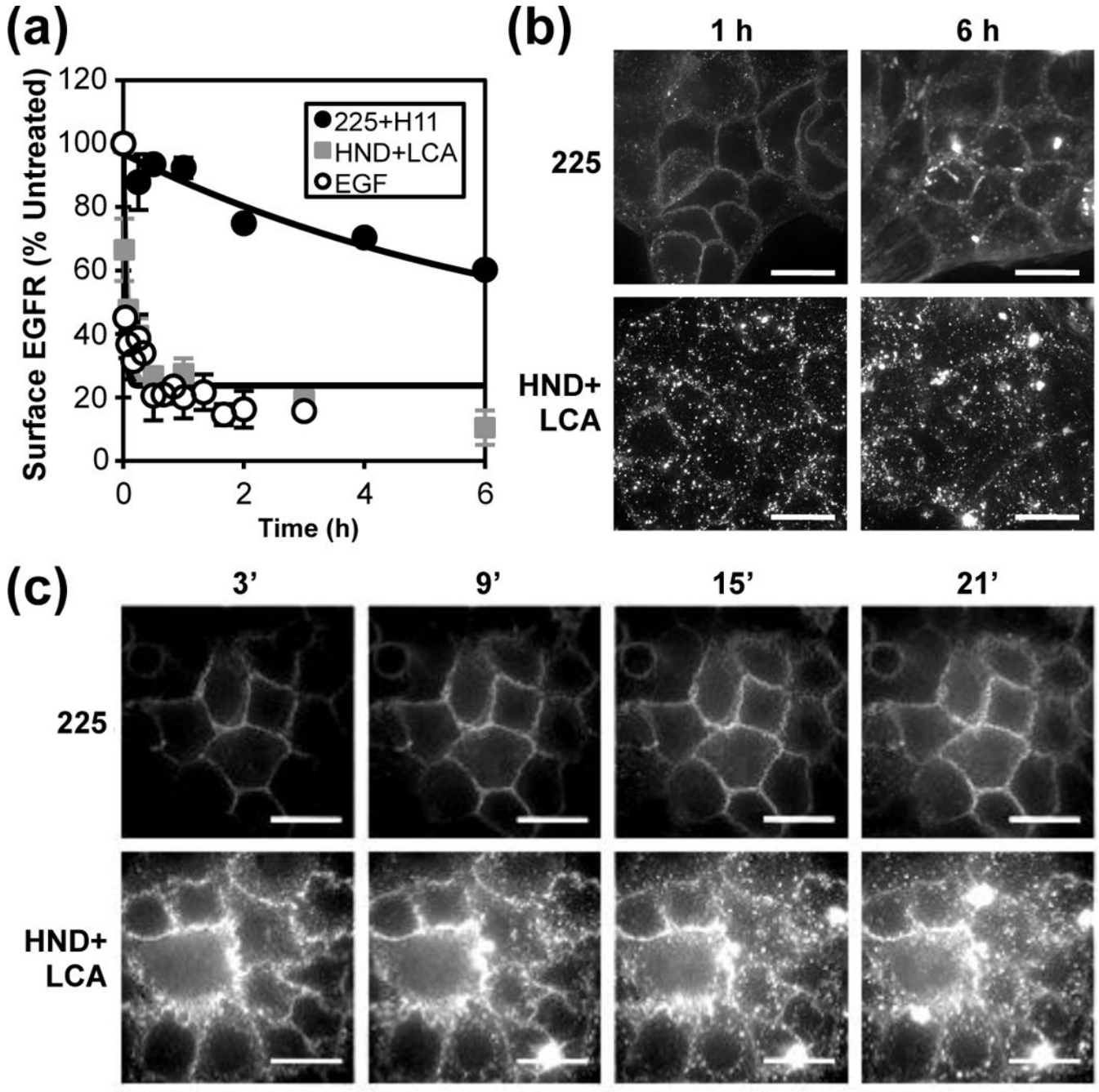

Fig. 3.

Ab-Fn3 fusion treatment rapidly induces internalization and clustering of EGFR. **(a)** HT-29 surface EGFR downregulation profile following treatment with an antibody cocktail (225+H11) ( ), the trans-tripepitopic Ab-Fn3 fusion HND+LCA ( ), or EGF ( ). Solid lines represent non-linear least squares regression fits to first-order kinetics. **(b)** Deconvolved images of HT-29 cells incubated with fluorescently-labeled antibody or Ab-Fn3 fusion for the indicated lengths of time. **(c)** Time lapse of A549 cells treated with fluorescently-labeled 225 or HND+LCA. Images reflect projections of 0.15 μm thick planes through the cell monolayer. All scale bars are of length 15 μm.

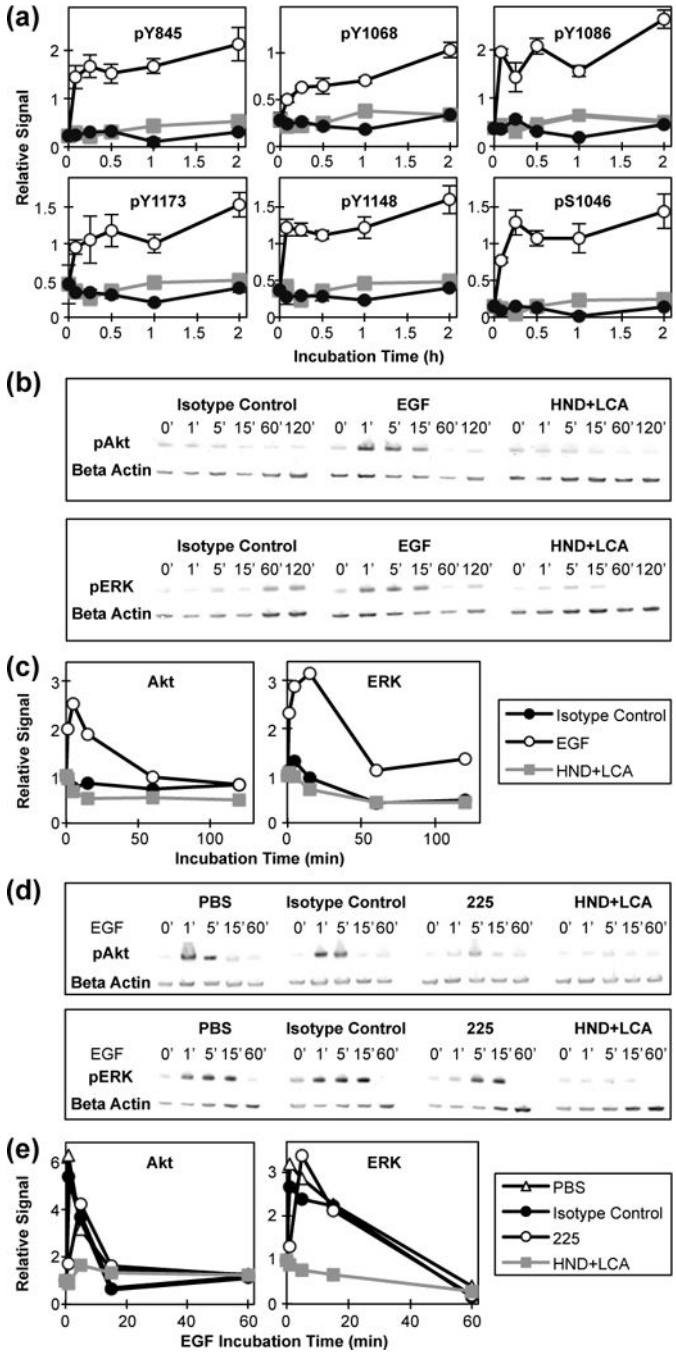

Fig. 4.

Ab-Fn3 fusion treatment does not activate EGFR and antagonizes downstream signaling through Akt and ERK. **(a)** In-cell western assays were performed on A431 cells for six established EGFR tyrosine and serine phosphosites. Activation profiles are shown for treatment with 20 nM human IgG1 isotype control antibody ( ), HND+LCA ( ), and EGF ( ). Phosphoprotein fluorescence was normalized by DNA fluorescence and signal relative to that of untreated cells is plotted versus time. **(b)** Immunoblot analysis of the phospho-Akt and phospho- ERK response to 20 nM isotype control antibody, EGF, and the trans-

triepitopic construct HND+LCA. HT-29 cells were incubated for the indicated length of time and assessed for stimulation of EGFR-driven effectors in the PI3K and MAPK pathways. **(c)** Quantification of the results presented in **(b)**. **(d)** HT-29 cells were incubated for 13 h with PBS or 20 nM human IgG1 isotype control antibody, 225, or HND+LCA. The cells were subsequently stimulated with 20 nM EGF for the indicated length of time and subjected to immunoblot analysis for quantification of phospho-Akt and phospho-ERK. **(e)** Quantification of the results presented in **(d)**. Band intensities were normalized by beta actin levels and by the intensity of a control lysate included on each blot.

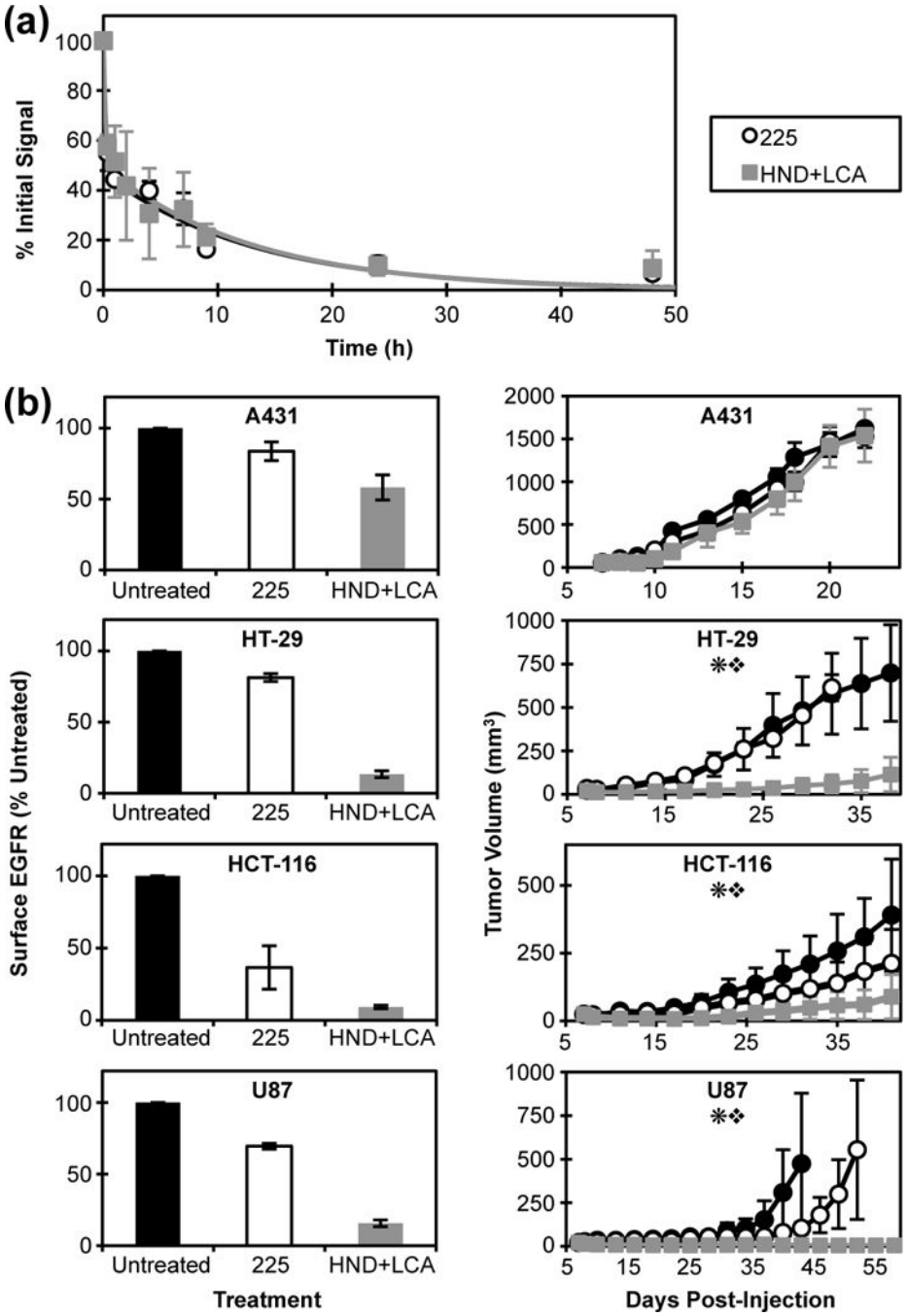

Fig. 5.

In vitro EGFR downregulation correlates with *in vivo* control of mouse tumor xenograft growth. **(a)** Clearance of 225 versus the trans-triepitopic fusion HND+LCA in athymic mice. Blood plasma levels of near-infrared dye-labeled 225 ( ) or HND+LCA ( ) were measured periodically for 48 h post-injection via tail vein bleeding. Fractional intensity relative to initial signal is presented at each time point with a biphasic clearance curve overlaid. **(b)** Cell surface EGFR downregulation (left) and *in vivo* tumor growth (right) following treatment with HND+LCA in four EGFR-expressing cell lines. For

downregulation assays, cells were treated with PBS or 20 nM 225 or HND+LCA for 13 h and analyzed for surface EGFR expression. For xenograft models, mice were treated every three days with PBS ( ) or 10 mg/kg 225 ( ) or HND+LCA ( ) beginning on day 7 post-tumor inoculation. The symbols ❋ and ❖ denote $P<0.05$ for the HND+LCA cohort versus the PBS and 225 cohorts, respectively, by one-way repeated measures ANOVA.

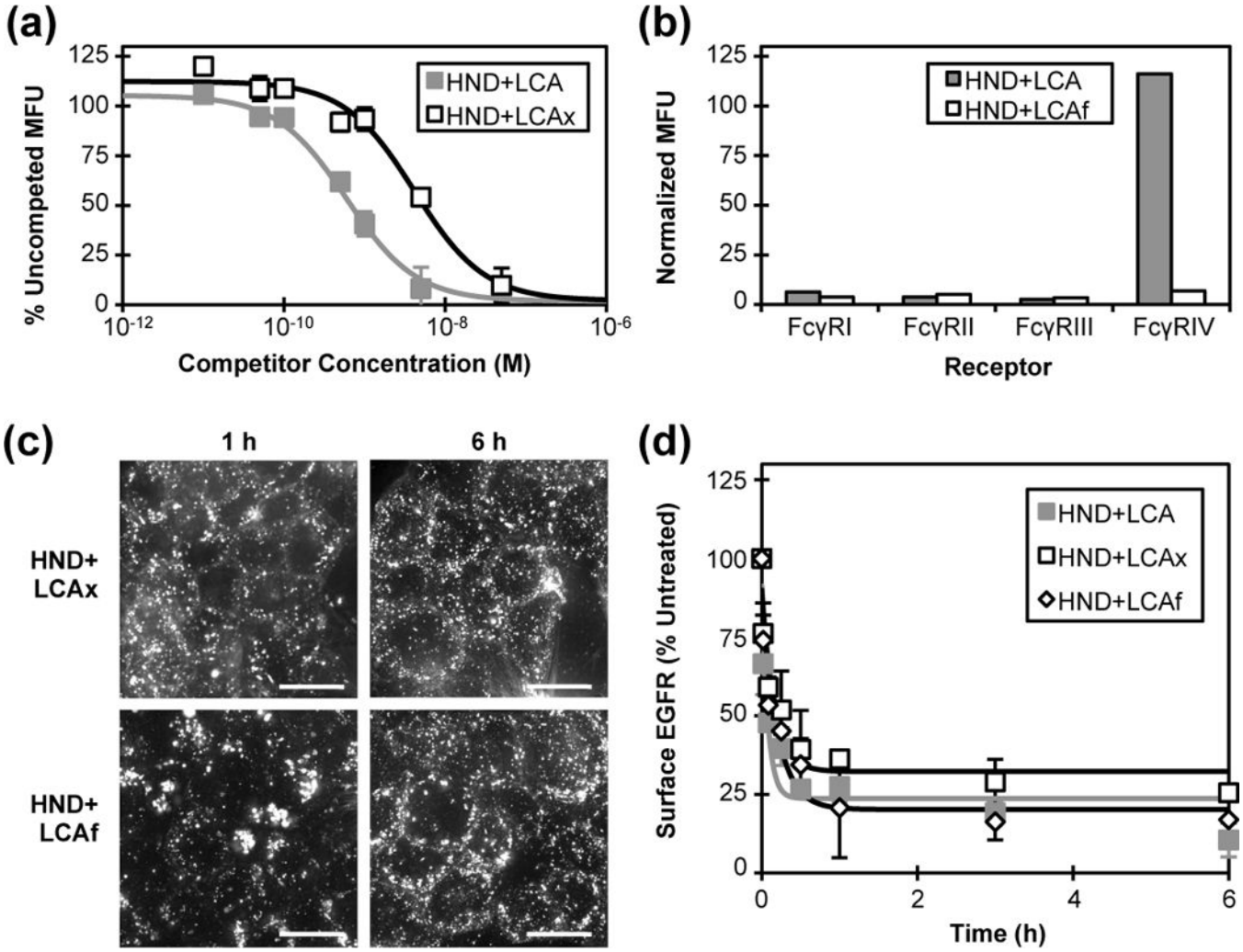

Fig. 6.

Introduction of mutations in the 225 heavy chain variable domain or the Fc domain isolate ligand binding and Fcγ receptor interaction, respectively, without significantly impacting EGFR clustering or downregulation extent. **(a)** Competition assays depicting EGF binding to HT-29 cells pre-incubated with the indicated concentrations of trans-triepitopic Ab-Fn3 fusion HND+LCA (★) or the 225 variable domain mutant HND+LCAx (✂). **(b)** Binding of HND+LCA or the Fc mutant HND+LCAf to yeast-displayed mouse Fcγ receptors I, II, III, and IV. **(c)** Deconvolved images of HT-29 cells incubated with 20 nM fluorescently-labeled HND+LCAx and HND+LCAf variants for 1 or 6 h at 37ºC. Projections of 0.15 μm slices through the full cell volume are presented. Scale bars = 15 μm. **(d)** Surface EGFR downregulation profiles of HT-29 cells treated with 20 nM HND+LCA (★) or the variants HND+LCAx (✂) or HND+LCAf (✎). Solid lines depict non-linear least squares regression fits to first-order kinetics. As shown, the 225 variable and constant domain mutations do not significantly alter downregulation kinetics nor do they affect the steady state level of surface receptor.

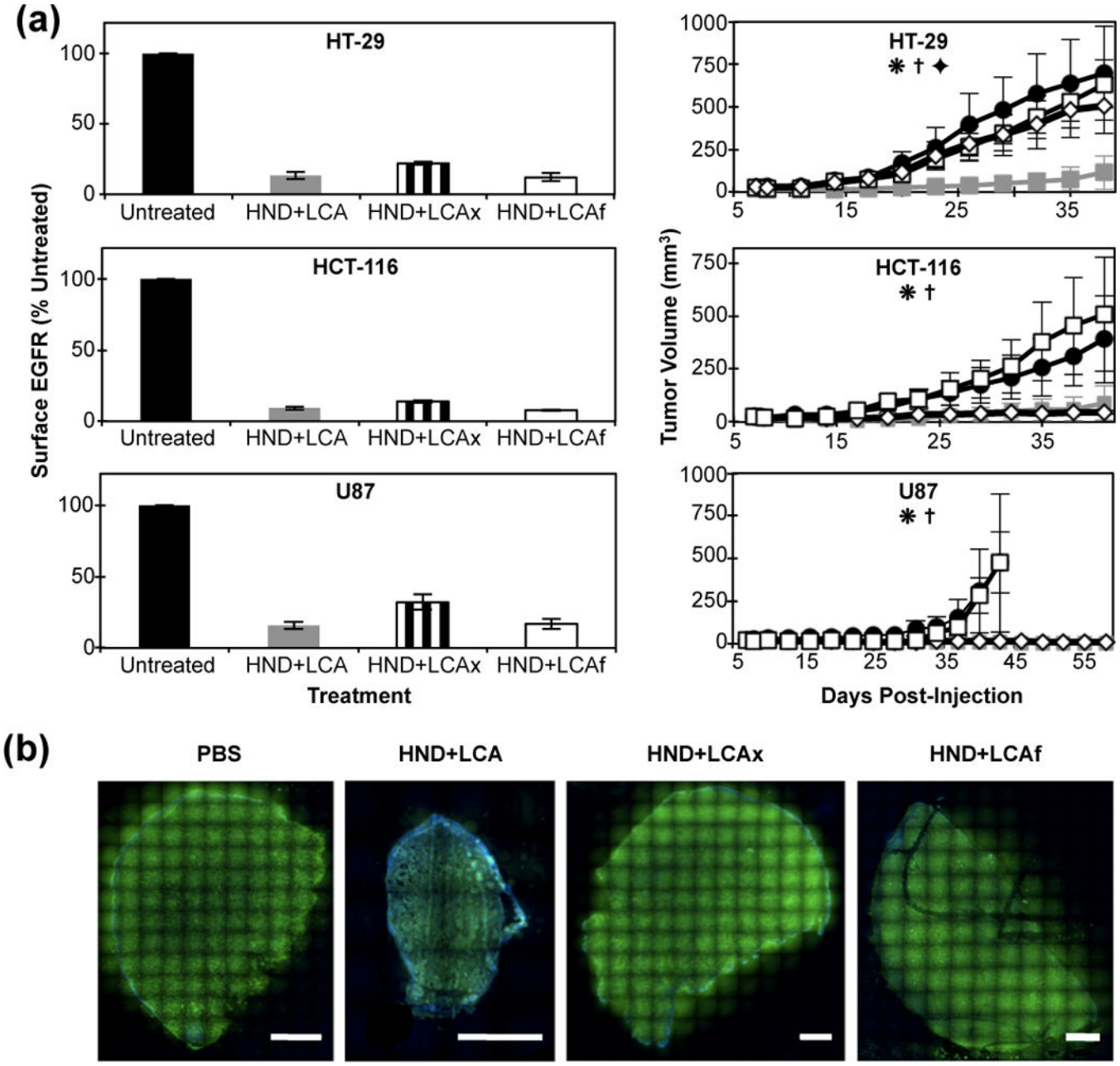

Fig. 7.

Downregulation, EGF competition, and immune effector function contribute to Ab-Fn3 fusion-mediated inhibition of mouse tumor xenograft growth in 225-resistant cell lines and tumor control coincides with reduced EGFR expression. **(a)** *In vitro* EGFR downregulation (left) and *in vivo* tumor xenograft growth (right) assays. For downregulation assays, cells were incubated with PBS or 20 nM 225, HND+LCAx, or HND+LCAf for 13 h and assessed for surface EGFR levels. For xenograft tumor studies, mice were dosed with PBS ( ) or 10 mg/kg HND+LCA ( ), HND+LCAx ( ), or HND+LCAf ( ) every three days beginning on day 7 post-tumor inoculation. The symbols ⁕, †, and ✦ denote $P<0.05$ for HND+LCA versus PBS, HND+LCAx, and HND+LCAf, respectively. Statistical analyses were

performed using a one-way repeated measures ANOVA algorithm. **(b)** Stitched images of EGFR levels in HT-29 tumor xenografts following treatment with PBS or 10 mg/kg HND +LCA, HND+LCAx, or HND+LCAf. HT-29 tumor xenograft-bearing mice treated every three days beginning on day 7 post-inoculation were sacrificed on day 38, 24 h after administration of the final treatment. Disected tumors were subsequently sectioned and immunofluorescently stained for human EGFR (green) and cell nuclei (blue). Both intracellular and extracellular EGFR is visible due to membrane permeabilization. Scale bars = 1 mm.

Table 1

Cell surface titration affinities of multiepitopic Ab-Fn3 fusions. Apparent equilibrium dissociation constants of well-expressed cis- and trans-triepitopic and HN biepitopic Ab-Fn3 fusion constructs on the surface of A431 cells at endosomal (6.0) or physiological (7.4) pH.

Construct	K_d, pH 6.0 (pM)	K_d, pH 7.4 (pM)
225	370	1284
HN-AD	1316	1264
HN-DB	122	1647
HNA+LCD	167	284
HNB+LCD	213	196
HND+LCA	25	71
HND+LCB	123	294
HN-A	191	237
HN-B	24	61
HN-D	40	75